

Amorphization in the vicinity of a grain boundary: A molecular-dynamics approach

Gonzalo Gutiérrez, Miguel Kiwi, and Ricardo Ramírez

Facultad de Física, Universidad Católica de Chile, Casilla 306, Santiago 22, Chile

(Received 25 May 1995; revised manuscript received 20 June 1996)

The dynamics of the melting process of a binary system (such as the one formed by Co and Zr) that contains a grain boundary is investigated by means of molecular dynamics using Lennard-Jones-type interatomic potentials. The evolution of the disordering sequence, as the temperature is increased, is quantitatively studied and graphically illustrated. It is found that the presence of the defect acts like a seed for the disordering, with the genesis of an intermediate amorphous phase. The latter is properly identified and characterized and constitutes an intermediate stage before the proper melting process sets in. [S0163-1829(96)04940-5]

I. INTRODUCTION

The role of defects in both melting and crystal growth processes has been of interest to condensed matter physicists for a long time.¹ Metallic glass formation through interdiffusion at an interface between two crystalline solids has also attracted the attention of physicists, metallurgists, and chemists.² In fact, after it was reported by Johnson and Schwartz,³⁻⁵ solid state amorphization has recently been investigated by several groups.⁶ Significant contributions to the understanding of the relation between amorphization and melting have been made using molecular dynamics, notably by Wolf *et al.*⁷ The special case of the amorphization of NiZr₂ was studied, with the use of molecular dynamics, by Massobrio, Pontikis, and Martin.⁸ On the experimental front, the metallic glass formation at a Zr-Co interface was studied by means of electron microscopy by Schröder, Samwer, and Koster.⁹

In this contribution we report on a molecular-dynamics study of the interplay between crystal defects and the disordering process generated by the increase of temperature, when the interface is located in the vicinity of a grain boundary. As is well known,¹⁰ several physical properties such as interdiffusion and impurity migration rates are strongly influenced by the presence of grain boundaries.^{11,12} On the other hand, the impurity concentration in the neighborhood of a grain boundary strongly influences the embrittlement of a polycrystalline sample. Consequently, non-negligible effects are to be expected from the interaction of crystal defects and the disordering process.

Molecular-dynamics studies seem well suited to tackle the problem at hand. In fact, as already pointed out by Pontikis,¹³ ordinary methods of solid state theory are of limited usefulness when faced with the strong perturbations of the electronic density of states in the vicinity of crystal defects. Moreover, the harmonic approximation cannot handle correctly the large-amplitude relaxations that occur around these defects. Finally, temperature effects are not easy to incorporate in the usual treatments. However, computer simulations in general and molecular dynamics in particular can provide some relevant information under these rather strained circumstances.

The procedure we implement follows closely along the lines outlined in the paper of Weissmann *et al.*,¹⁴ who stud-

ied the amorphization process of a flat Co-Zr-like interface. However, the Lennard-Jones interaction potential adopted is too simple to describe transition-metal alloys and compounds. Thus when we speak of Co and/or Zr we only do so in a generic sense, intending to illustrate the general behavior of systems with two different but spatially contiguous atomic elements, which have the atomic size and melting temperatures of Co and Zr, respectively. Hence our results do not pretend to rigorously model the Co-Zr system, but rather apply to a class of systems dominated by size effects, of which Co-Zr may (or may not) be an example.

The results of Ref. 14, quite independently of the details of the boundary conditions and/or the two-body potentials used, demonstrated that (i) as the temperature T increases surface amorphization at the interface develops, while the bulk remains periodic; (ii) upon a further increase in temperature the disorder spreads towards the bulk; and (iii) finally, for even higher values of T , the whole system melts. Thus the main purpose of the present contribution is to investigate how the above-sketched results are modified by the presence of a grain boundary. A rather complex "tricrystal" geometry, with a tilt boundary and an interface, is adopted. Since interdiffusion rates in the vicinity of a grain boundary are known to be much larger than in the bulk,¹⁵ one expects these lattice defects to play a significant role on the disordering dynamics, as the sample is heated.

This paper is organized as follows. After this introduction the model we adopt is precisely defined in Sec. II. The results of the computations are presented in Sec. III. The paper concludes in Sec. IV, where the results are discussed and conclusions are drawn.

II. MODEL

The system consists of a cell containing 4037 atoms, of which 2511 represent Co and 1526 represent Zr. Both elements, initially in a fcc configuration, are arranged as displayed in Fig. 1(a). The Zr subcell contains a symmetric grain boundary in the y - z plane. For the purpose at hand we have chosen a $36.9^\circ \Sigma=5$ (031) tilt boundary, which lies on the (031) plane.¹⁶ A tricrystal is generated in this way since we are in the presence of a symmetric tilt grain boundary within the Zr region plus a tilt boundary between Zr and Co.

In these simulations special attention has to be given to a

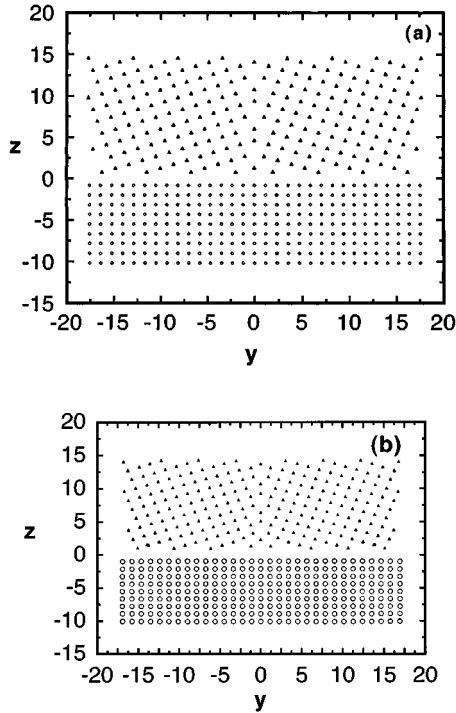


FIG. 1. Projection of all the atomic positions onto the y - z plane, for (a) $T=0$ and (b) the initial minimum-energy configuration, obtained from (a) by conjugate gradient searches, at $T=0$. The Co and Zr atoms are denoted by open circles and full triangles, respectively.

crucial issue: the proper choice of the boundary conditions. In our case periodic boundary conditions can be imposed only in the x direction, which is the single axis with translation invariance. In the y and z directions the problem is far more complicated, as the simulation cell has to be properly immersed into the bulk. Here several alternative ways have been put forth, which range from clamping the cell boundary atoms to attaching them to a completely mobile rigid slab. We have adopted a compromise: we allow the boundary atoms to oscillate around their initial equilibrium positions with a frequency determined by the harmonic part of the potential. The initial phase of these Einstein oscillators is chosen at random. This way, without fully escaping finite-size effects, we adopt a better approximation than imposing fixed boundary conditions.

Another major issue in molecular-dynamics computations is the adequate choice of the interaction potential.^{17,18} As in Ref. 14, we adopt the two-body interaction

$$V(r) = \frac{A_\alpha}{r^4} + \frac{B_\alpha}{r^8} + C_\alpha r + D_\alpha, \quad (2.1)$$

where $\alpha = \text{Zr}$ or Co and the parameters C and D were included in order to allow for a smooth potential cutoff.¹⁸ In fact, they were chosen so that the potential goes to zero, with zero gradient, at $r=2d$, where d is the position of the minimum of $V(r)$. Since the first-, second-, and third-neighbor distances are d , $\sqrt{2}d$, and $\sqrt{3}d$, respectively, this implies that the potential is of third-nearest-neighbor range. In addition, the curvature of the potential at the minimum is determined

by fitting the experimental value of the respective bulk modulus. The parameters A , B , C , and D are fully determined by these requirements, plus fitting the melting temperatures and atomic sizes of Co and Zr. For the interaction between Co and Zr atoms we have taken the geometric average of the parameters of the pure materials. Further details on the choice of the potential can be found in Ref. 14.

III. RESULTS

The molecular-dynamics (MD) simulations were implemented, for up to 30 000 time steps in every run, according to the scheme outlined in Sec. II. The time step we adopted is of 4.4×10^{-15} s, our unit of length is 1.5486 Å, and the temperatures are reported in units of ≈ 5400 K. Our interest is to trail closely the disordering process, which we do by slowly increasing the temperature. Thus we start with a normal (Maxwellian) velocity distribution at a low-temperature value and increment the total energy by boosting the velocities in small steps.

The starting atomic arrangement is the one displayed in Fig. 1(a). However, this system is not the equilibrium configuration, even at $T=0$. An improved minimum-energy configuration was consequently generated after extensive conjugate gradient searches at $T=0$. It is illustrated in Fig. 1(b) and constitutes the starting point of all our molecular-dynamics simulations. It is quite clear that Figs. 1(a) and 1(b) are quite similar; actually, the main difference is a slight shrinking in the y and z directions.

Moreover, we confirmed that this new grain boundary is stable against rigid translations of the two grain halves relative to each other. To reach this conclusion we shifted rigidly one side of the starting grain boundary, relative to the other, along the z direction. This shift amounted to up to 6% of the Zr lattice parameter and was implemented in steps of 2% of this parameter. After each 2% shift conjugate gradient searches at $T=0$ were carried out. For these displacements the energy minimization procedure leads the system back to the initial configuration illustrated in Fig. 1(b). It is worth mentioning that shifts in the z direction are equivalent to the removal of a Zr atom plane parallel to the grain boundary, followed by the corresponding rigid body translation.

Moreover, we confirmed that the energy differences associated with these z translations are very small when compared with the energy differences related to the introduction of the Co-Zr interface, which is the focus of interest of this paper. In addition, we confirmed that mirror image related atoms in the Zr bulk do not shift in the z direction relative to each other, as a consequence of the molecular-dynamics runs. The same holds for the x direction, where periodic boundary conditions impose severe constraints.

Here we are mainly interested in what happens to the Co as a consequence of the grain boundary in the Zr. A most direct and convenient way to analyze disorder is simply to display graphically the particle distributions, for example, to display particle spatial positions and to plot the number of particles between z and $z+dz$. However, some quantification of the degree of disorder is also obtained through the evaluation of the structure factor, the pair correlation function, and the mean-square atomic deviation.

The static structure factor, i.e., the Fourier transform of

the density in each crystallographic Co plane, is calculated¹⁶ as a convenient way of characterizing the degree of order in the plane. It is defined by

$$S(\vec{K}, n) = \left\langle \frac{1}{N_z^2} \left| \sum_{j=1}^{N_z} \exp(i\vec{K} \cdot \vec{r}_j) \right|^2 \right\rangle, \quad (3.1)$$

where n labels the crystal plane to which the N_z lattice points \vec{r}_j belong at low temperatures and \vec{K} is a vector of the planar reciprocal lattice.

Another probe of the disorder is to calculate $g_2(r)$, the pair correlation function.¹⁴ Still another way to characterize disorder, this time dynamically, is to evaluate the mean-square deviation from the initial configuration $\langle (r - r_0)^2 \rangle$. The average slope of this parameter versus the number of molecular-dynamics steps is related to the diffusion coefficient.

A relevant issue to ascertain the internal consistency of our results is the determination of the Co thermodynamic melting temperature T_m^{Co} of our simulation model. In principle, the temperature-dependent free energies of the perfect solid and of the liquid should be obtained; the thermodynamic melting temperature T_m is defined as the temperature at which the free energy of the crystalline and liquid phases are equal. While free-energy analysis is possibly the best choice, it is not easy to implement.¹⁹ Almost as good, but much easier to perform, is to determine the propagation velocity of the solid-liquid interface versus temperature and extrapolate to zero velocity, as done by Lutsko and Wolf in Ref. 20. The basic idea is to carry the system illustrated in Fig. 1(b) to a high temperature, well above the melting point, and to determine how the melting front propagates as a function of time (actually, MD steps). The particular parameter chosen to characterize the melting dynamics is the number of “defected” atoms, which are defined as those with a nearest-neighbor coordination different from that of the ideal crystal environment. Full details on the procedure, which we used to determine T_m^{Co} , can be found in Refs. 19 and 20.

On the other hand, it is known that the values obtained for T_m are smaller than the ones obtained through simulations in an ideal crystal cell with periodic boundary conditions, a phenomenon known as superheating. In our case the grain boundary acts as a nucleation center⁷ and thus what we de-

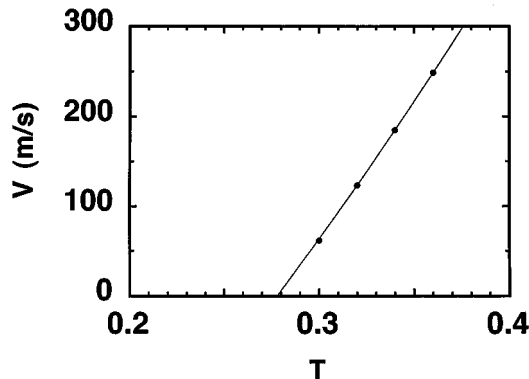


FIG. 2. Velocity of propagation v , of the Co solid-liquid interface, as a function of temperature T . The extrapolation to zero velocity is obtained by means of a quadratic fit to the data points.

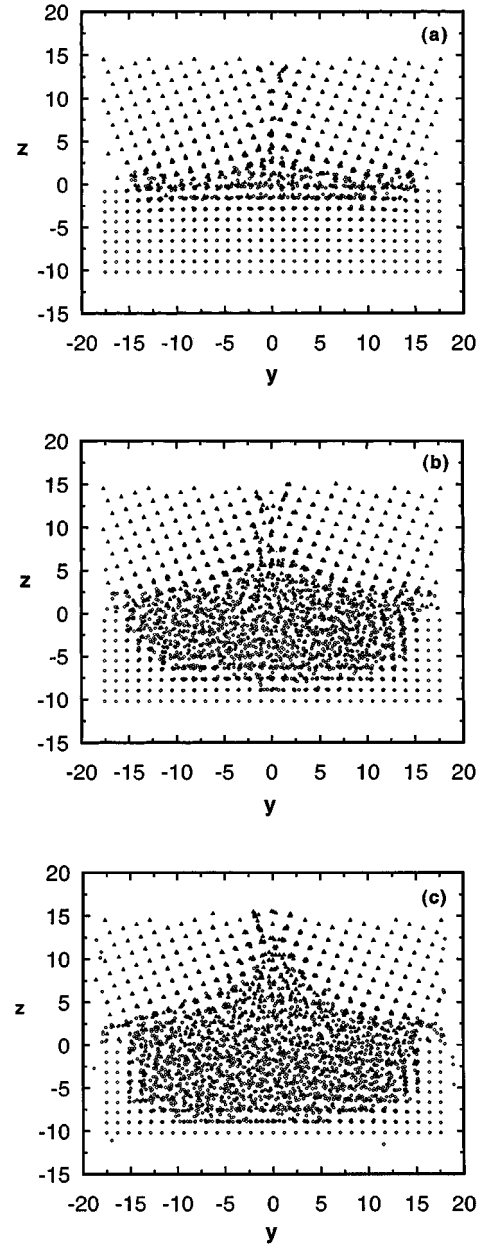


FIG. 3. Same as Fig. 1, but for (a) $T=0.15$, (b) $T=0.24$, and (c) $T=0.28$.

termine is the thermodynamic melting temperature T_m . The results we obtained for the melting front propagation velocity are displayed in Fig. 2, where the data were fitted with a quadratic polynomial to obtain the value of $T_m^{\text{Co}} \approx 0.28$. It is important to notice that this value of T_m^{Co} is lower than the one obtained when superheating an isolated perfectly crystalline sample of Co, for which one obtains a melting temperature $0.32 \leq T \leq 0.34$.

As the system is heated it evolves as illustrated in Fig. 3. In fact, as the temperature is increased, first to $T=0.15$ [Fig. 3(a)] and then to $T=0.24$ [Fig. 3(b)], the system undergoes a very significant change. When the temperature $T=0.28$ [Fig. 3(c)] is finally reached, the original grain boundary has all but disappeared.

The most important observation, related to these results, is

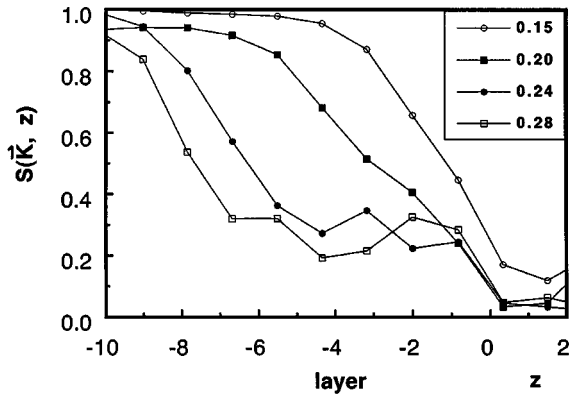


FIG. 4. Structure factor $S(\vec{K}=(1,1),z)$ versus layer index for the four different temperature values specified in the inset.

that first the interface and then the “bulk” Co become completely disordered. Of course this disordering is related to the lower melting point of Co relative to Zr, but the phenomenon is strongly enhanced by two factors: (i) the lattice parameter mismatch, due to the different sizes of the two atomic species in the system, and (ii) the presence of the grain boundary. This is borne out as well by the structure factor $S(\vec{K},z)$ of Eq. (3.1), plotted versus the layer index in Fig. 4, for five different values of the temperature. A clear-cut change is observed at $T=0.24$, when the low interface value of $S(\vec{K},z)<0.2$ spreads into the sample. This is to be contrasted with the flat interface results of Ref. 14, where a similar behavior was observed, but at higher temperatures.

The overall picture outlined above is reinforced by the pair correlation function results, used as a crucial probe by Massobrio *et al.*⁸ They are plotted in Fig. 5 for the same temperature values of Fig. 3. It is observed that for each of these values ($T=0.15$, $T=0.24$, and $T=0.28$) a qualitatively

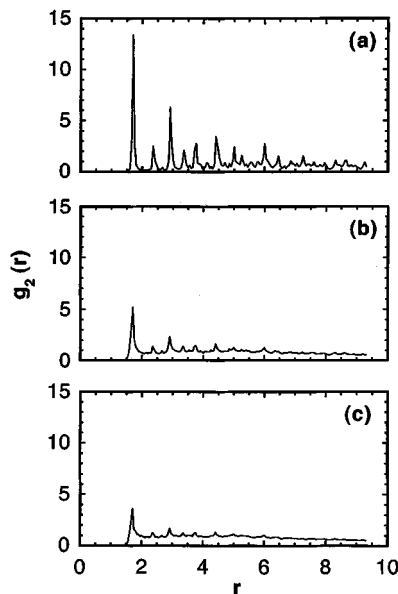


FIG. 5. Pair correlation function versus distance for (a) $T=0.15$, (b) $T=0.24$, and (c) $T=0.28$.

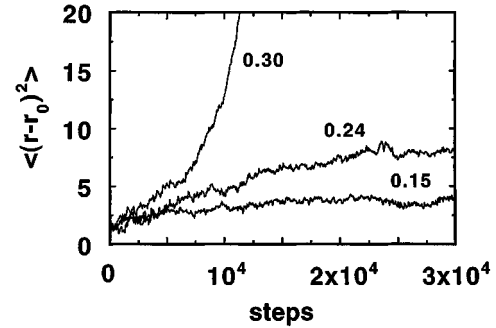


FIG. 6. Mean-square deviation versus number of molecular-dynamics steps.

different result is obtained. We claim that they correspond to an ordered, an amorphous, and a liquid phase, respectively. This assertion is consistent with all the above-mentioned results and with Ref. 14.

Moreover, this point of view is reinforced by Fig. 6, where the mean-square deviation $\langle(r-r_0)^2\rangle$ of the initial positions versus the number N of molecular-dynamics steps is represented, and by Fig. 7, where the total versus kinetic energy is plotted. Both of these graphs show distinct low- ($T<0.2$), intermediate- ($0.2<T<0.28$) and high- ($T>0.3$) temperature behavior. The average slope of $\langle(r-r_0)^2\rangle$ in Fig. 6 allows us to estimate the diffusion coefficient D ; we obtain $D\approx 6\times 10^{-12}$ m²/s for $T=0.15$, $D\approx 1.4\times 10^{-10}$ m²/s for $T=0.24$, and $D\approx 3.2\times 10^{-9}$ m²/s for $T=0.3$, which are acceptable for the solid, amorphous, and liquid phases, respectively. Also in Fig. 7 three different regimes are quite apparent. Both a change in slope at $T=0.2$ and a discontinuous transition between $T=0.28$ and $T=0.30$ are clearly noticeable.

Finally, in Fig. 8 the potential energy versus the number of steps, for three different temperatures, is presented. For $T=0.15$ and $T=0.24$ it is observed that the potential energy remains constant, which is consistent with localized interface disorder, which does not propagate into the bulk. This strengthens the case for interface amorphization, in contrast to a propagating liquid-solid interface. On the other hand, for $T=0.30$ the absolute value of the potential energy decreases as a function of time, as expected in the presence of a propagating liquid-solid interface.

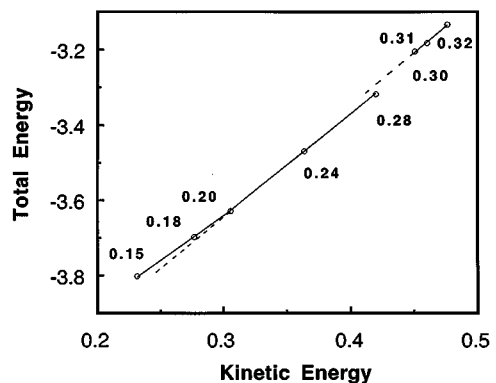


FIG. 7. Total energy versus kinetic energy. The numbers on the graph denote temperature values.

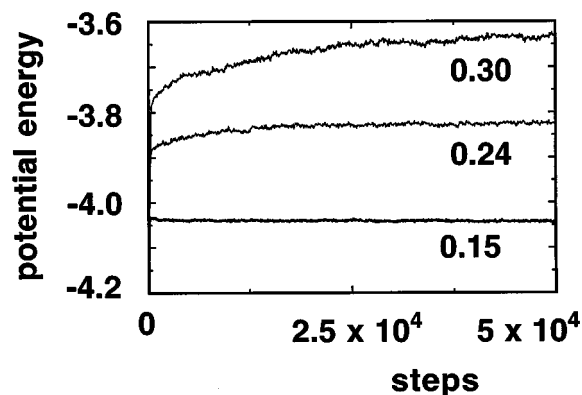


FIG. 8. Potential energy versus number of molecular-dynamics steps, for three different temperatures.

All in all a consistent description emerges in which the grain boundary facilitates the disordering process in its immediate vicinity. Moreover, an intermediate stage is identified and characterized as an amorphous phase, which plays the role of a precursor to the melting process proper.

IV. DISCUSSION AND CONCLUSION

In summary, we have implemented a Lennard-Jones molecular-dynamics simulation of a binary system, where

we model two atomic elements that have the atomic size and melting temperatures of Co and Zr, respectively. Our system contains a $36.9^\circ \Sigma=5$ (031) tilt grain boundary. While the crudeness of the Lennard-Jones treatment does not allow us to fully model the metallic Co-Zr system, we expect to have computed the right physical trends.

We interpret our results to portray an order-disorder transition in which the interface and the grain boundary act as a seed for the disordering process. Within the present limitations of molecular dynamics, both in system size and computer time, the overall understanding that emerges is of a fusion process that proceeds via interface amorphization. The latter is facilitated and enhanced by the presence of the grain boundary.

ACKNOWLEDGMENTS

We gratefully acknowledge enlightening conversations with Dr. Mariana Weissmann and Dr. Jinghan Wang. Supercomputer time was provided by the University of California-San Diego Supercomputer Center. This work was supported by the Fondo Nacional de Investigaciones Científicas y Tecnológicas (FONDECYT, Chile) under Grant No. 1940699 and the Fundación Andes. G.G. was supported by CONICYT and by FONDECYT under Grant No. 2940022.

¹See, for example, *Les Joints de Grains dans Les Materiaux*, edited by M. Aucouturier (Les Editions de Physique, Paris, 1984).

²Proceedings of the Conference on Solid State Amorphizing Transformations, Los Alamos, 1987, edited by R. B. Schwartz and W. L. Johnson [*J. Less-Common Met.* **140**, (1988)].

³R. B. Schwartz and W. L. Johnson, *Phys. Rev. Lett.* **51**, 415 (1983).

⁴R. B. Schwartz, K. L. Wong, W. L. Johnson, and B. M. Clemens, *J. Non-Cryst. Solids* **61&62**, 129 (1984).

⁵B. M. Clemens, W. L. Johnson, and R. B. Schwartz, *J. Non-Cryst. Solids* **61&62**, 817 (1984).

⁶See, for example, *J. Phys. (Paris) Colloq.* **51**, C4 (1990).

⁷D. Wolf, P. R. Okamoto, S. Yip, J. F. Lutsko, and M. Kluge, *J. Mater. Res.* **5**, 286 (1990).

⁸C. Massobrio, V. Pontikis, and G. Martin, *Phys. Rev. Lett.* **62**, 1142 (1989).

⁹H. Schröder, K. Samwer, and U. Koster, *Phys. Rev. Lett.* **54**, 197 (1985).

¹⁰J. Q. Broughton and G. H. Gilmer, *Phys. Rev. Lett.* **56**, 2692 (1986).

¹¹G. Martínez, M. Kiwi, and R. Ramírez, *Acta Metall.* **34**, 1583 (1986).

¹²G. Martínez and M. Kiwi, *Phys. Rev. B* **42**, 5527 (1990).

¹³V. Pontikis, in *Les Joints de Grains dans les Materiaux* (Ref. 1), p. 149.

¹⁴M. Weissmann, R. Ramírez, and M. Kiwi, *Phys. Rev. B* **46**, 2577 (1992).

¹⁵F. Dymont, M. J. Iribarren, K. Vieregge, and Chr. Herzig, *Philos. Mag.* **63**, 959 (1991).

¹⁶S. R. Phillpot, S. Yip, and D. Wolf, *Comput. Phys.* **3**, 20 (1989).

¹⁷F. H. Streitz, K. Sieradzki, and C. Cammarata, *Phys. Rev. B* **41**, 12 285 (1990).

¹⁸S. J. Plimpton and E. D. Wolf, *Phys. Rev. B* **41**, 2712 (1990).

¹⁹J. F. Lutsko, D. Wolf, S. R. Phillpot, and S. Yip, *Phys. Rev. B* **40**, 2841 (1989).

²⁰J. F. Lutsko and D. Wolf, *Scr. Metall.* **22**, 1923 (1988).